

The paper presents studies of the system "induction generator-induction motor" with parametric asymmetry on a mathematical model to determine the quality of generated electricity in load operating modes. A mathematical model of the "induction generator-induction motor" system has been developed taking into account losses in steel and parametric asymmetry. The analysis of the transient characteristics of an induction generator when a motor load is connected in symmetrical and asymmetrical modes of operation is carried out. The results of changes in the main characteristics of an induction motor at various degrees of parametric asymmetry in the generator are presented. The quality of the generated electricity was analyzed based on the calculations of the unbalance coefficients for each of the operating modes. The assessment of the thermal state in steady-state conditions was carried out using an equivalent thermal equivalent circuit. Thermal transients were investigated when starting an induction motor from an autonomous energy source based on an induction generator. On a thermal mathematical model, the study of the effect of the output voltage asymmetry on the heating of the connected induction motor was carried out. It is shown that the asymmetry of the output voltage of an induction generator reaches 3–10 % and causes overheating of the windings in excess of the permissible values. A regression model has been developed for studying the operating conditions of an induction motor when powered by an induction generator with an asymmetry of the stator windings. The use of the obtained equations will make it possible to determine the most rational combination of factors affecting the heating of the stator windings of induction machines, in which they will not overheat above the maximum permissible temperature values of the corresponding insulation classes

**Keywords:** induction generator, induction motor, mathematical model, hodograph, thermal model, regression analysis

UDC 621.45.778

DOI: 10.15587/1729-4061.2021.239146

# DEVELOPMENT OF MATHEMATICAL MODELS OF ENERGY CONVERSION PROCESSES IN AN INDUCTION MOTOR SUPPLIED FROM AN AUTONOMOUS INDUCTION GENERATOR WITH PARAMETRIC NON-SYMMETRY

**Volodymyr Chenchevoi**

PhD, Associate Professor\*

**Valeriy Kuznetsov**

Doctor of Technical Sciences, Professor

Electric Power Department

Railway Research Institute

Chlopickiego str., 50, Warsaw, Poland, PL 04-275

**Vitaliy Kuznetsov**

Corresponding author

PhD, Associate Professor

Department of Electrical Engineering

National Metallurgical Academy of Ukraine

Gagarina ave., 4, Dnipro, Ukraine, 49600

E-mail: wit\_jane2000@i.ua

**Iurii Zachepa**

PhD, Associate Professor\*

**Olga Chencheva**

PhD, Associate Professor

Department of Labor Protection, Civil and Industrial Safety\*\*

**Oleksii Chorny**

Doctor of Technical Sciences, Professor\*

**Maksim Kovzel**

PhD, Associate Professor

Iron and Steel Institute of Z. I. Nekrasov National Academy of Sciences of Ukraine

Akademika Starodubova sg., 1, Dnipro, Ukraine, 49107

**Viktor Kovalenko**

Doctor of Technical Sciences, Professor\*\*\*

**Mykola Babyak**

PhD, Associate Professor

Department of Transport Technologies

Dnipro National University of Railway Transport named after Academician V. Lazaryan

Lazaryana str., 2, Dnipro, Ukraine, 49010

**Serhii Levchenko**

PhD, Associate Professor\*\*\*

\*Department of Automatic Control Systems and Electric Drive\*\*

\*\*Kremenchuk Mykhailo Ostrohradskyi National University

Pershotravneva str., 20, Kremenchuk, Ukraine, 39600

\*\*\*Department of Electrical Engineering and Energy Efficiency

Zaporizhzhia National University

Zhukovskoho str., 66, Zaporizhzhia, Ukraine, 69600

Received date 09.07.2021

**How to Cite:** Chenchevoi, V., Kuznetsov, V., Kuznetsov, V., Zachepa, Y., Chencheva, O., Chorny, O., Kovzel, M., Kovalenko, V., Babyak, M., Levchenko, S.

Accepted date 23.08.2021

(2021). Development of mathematical models of energy conversion processes in an induction motor supplied from an autonomous induction generator with

Published date 31.08.2021

parametric non-symmetry. *Eastern-European Journal of Enterprise Technologies*, 4 (8 (112)), 67–82. doi: <https://doi.org/10.15587/1729-4061.2021.239146>

## 1. Introduction

The development of agriculture leads to an increase in demand for autonomous power supplies (APS). This is pri-

marily due to insufficient reliability of centralized power supply and quality of electricity, which, in turn, disrupts technological processes and causes losses caused by shortages and losses of agricultural products.

Induction generators (IG) are widely used as APS [1–4]. The advantages of IG are manufacturability, simplicity of design, autonomy, lack of contacts, reliability, ease of use. AGs allow them to be used in a wide variety of areas of the national economy. Such generators are used to power hand-held power tools with a built-in high-frequency electric drive, when taking power from the main power plant in the electric power systems of transport facilities.

The main power collectors in agriculture are electric drives, which make up 66...74 %. The peculiarities of the power supply of various technological processes in the agricultural sector is the remoteness or lack of centralized power supply (work in the field, power supply of agricultural electrotechnical installations, power tools, etc.).

The operating modes of autonomous power supplies are characterized by sharply changing loads and require the use of specialized equipment. This is especially true of cases when a direct start of induction squirrel-cage motors of comparable power is carried out from an autonomous source. Significant inrush currents affect a decrease in the voltage on the buses of an autonomous source. Without taking special measures, stable operation of consumers connected in parallel with induction motors (IM) of comparable power becomes impossible, and the electric motors that turn on accelerate very slowly or do not start at all.

In this regard, the issue of using the IG as a source for powering the network, which includes the IM, is relevant. However, despite numerous works [5–8] devoted to theoretical and practical studies of hypertension in feeding IM, some issues have not been fully studied. In particular, there are no relevant studies of transient processes that would consider the effect of asymmetry in the windings of induction machines on their characteristics and operating modes.

During the IM operation, its parameters may deviate from the passport ones due to various damages [9–11]. The main causes of such malfunctions are motor vibration, overheating and mechanical stress. These factors lead to the appearance of electrical and magnetic asymmetry of the motor [12–14]. The violation of the IM symmetry can be caused by various damages of the windings and the core of the stator and the rotor, the occurrence of eccentricity of the rotor. Unbalance in the stator windings can appear as a result of damage such as breaks in parallel branches and elementary conductors of phase windings. Most often, such damage is the result of insulation breakdowns and the occurrence of turn circuits. As a result, harmonics of various orders appear in the field curve, which cause distortion of the shape of the torque curves and, with a significant proportion of the removed sections, can make it impossible to IM start.

---

## 2. Literature review and problem statement

---

In [15], the results of studies of the operation of an induction generator on a network with a motor load are given and the conditions for starting and the maximum power of the motor being switched on are indicated. It is shown that in the IG network, with an increase in the capacitor capacity, it is possible to start IM with a power of no more than 40 % of the generator power. But there were still unresolved issues related to the determination of the thermal state of IM when powered by hypertension. In [16], studies of the temperature characteristics of the IG were carried out in accordance with the distribution of losses in the stator. However, there

are no studies of the thermal state of the connected load, in particular, the IM.

In scientific works on this topic, the issues of the thermal state of the IM when powered from the IG in asymmetric modes of operation are practically not considered. Most of the works are devoted to the development of methods for calculating and analyzing the thermal state of an IM, considering the temperature characteristics of motors under various asymmetric operating modes associated with malfunctions of electric motors. So, in [17], the results of theoretical studies of asymmetry, dips and voltage surges at the IM are presented using the traditional method based on the theory of symmetric components. For this study, a mathematical model has been developed to calculate currents, torque, power losses, temperature rise and derating factor. Similarly, [18] discusses in detail the thermal analysis of IM when operating under these two conditions: unbalanced supply voltage and the presence of turn-to-turn short circuit. In this work, the finite element method was applied to generate fault scenarios, and software was used to simulate the electromagnetic and thermal behavior of the machine for varying degrees of severity of the aforementioned faults. In [19], a method is presented to compensate for the influence of the asymmetry of the stator windings of an induction motor on the characteristics of electric drive systems with vector control. Analysis of the orthogonal components of the electromagnetic torque in an analytical form showed that the effect of breaks causing the asymmetry of the stator circuits of an induction motor on the operating mode of the electric drive can be compensated by reducing the asymmetric flux linkage of the phases. In [20], an assessment of the adequacy of the thermal model of an induction motor operating under conditions of low-quality electricity was carried out, based on the results of an industrial experiment. In [21], an analysis of the mechanical, electromechanical and thermal characteristics of an induction motor in asymmetric modes of operation is carried out. A qualitative assessment of the possibility of further operation of the motor in case of supply voltage unbalance with different unbalance coefficients has been carried out.

In all the cases mentioned, the mathematical description was obtained when the IM was supplied from the mains. However, the study of electromagnetic processes and the determination of the thermal state of the IM when powered by the IG under various asymmetric modes of operation were not considered in any of the above works. Also, there are no universal models that comprehensively reflect the processes of converting energy into IM with multifactorial variations in operating and design parameters. Therefore, specialized mathematical models that correspond to individual processes are usually considered [12, 22, 23].

Thus, the issues of determining the thermal state of the IM when changing the parameters of the windings and the system of capacitor excitation of the IG remain insufficiently studied.

---

## 3. The aim and objectives of research

---

The aim is to develop mathematical models of autonomous power supplies based on induction generators to improve the reliability and efficiency of autonomous power supply for agricultural consumers.

This will make it possible to correctly configure the systems of a variable induction electric drive when powered

from energy sources with induction generators, taking into account the asymmetry of their characteristics and to increase their service life.

To achieve the aim, the following objectives were set:

- development of a mathematical model of an autonomous induction generator with capacitor excitation, taking into account losses in steel and parametric asymmetry in the stator windings;
- to analyze the electromechanical and starting characteristics of the motor when powered by an induction generator, taking into account the parametric asymmetry in the stator windings;
- to develop a thermal model of the “induction generator-induction motor” system with asymmetry in the stator windings;
- to develop a regression model that makes it possible to assess the influence of the asymmetry of the stator electrical circuit on the operation of induction machines.

---

#### 4. Materials and methods of research

---

An unfavorable confluence of climatic conditions or anthropogenic circumstances can lead to the creation of emergency situations due to a disruption in the power supply of industrial and municipal facilities. First of all, it is about various institutions of urgent medical care, heating systems and water supply and sewerage systems, the long-term lack of power supply of which can entail serious or even tragic consequences. The solution to the problem lies in the use of APS based on IG with capacitor excitation. One of the directions for further development with the APE use on the basis of IG is the study of electromagnetic and electromechanical processes and modes of operation of the IG when feeding the IM in the case of various malfunctions.

To study the electromagnetic and electromechanical processes at various operating modes in the IG and IM, a mathematical description of the dynamic modes of electrical machines in a three-phase coordinate system was used. Mathematical models of induction machines were implemented in the Simulink visual simulation program from the MATLAB package. The following initial data for the IG were selected:  $P_{nom}=7.5$  kW;  $p=2$ ;  $I_{nom}=14.6$  A;  $n_{nom}=1430$  rpm;  $\cos\phi_{nom}=0.825$ ;  $\eta_{nom}=81$  % and parameters of the equivalent circuit  $r_s=1$   $\Omega$ ;  $r_r=0.77$   $\Omega$ ;  $L_{ss}=0.008$  H;  $L_{rs}=0.009$  H;  $L_\mu=0.366$  H;  $C=200$   $\mu$ F. To estimate the maximum IG power required for direct start of an induction squirrel-cage electric motor and study its operation in a steady state, an AOLS2–21–4 electric machine (USSR, developed in 1957–59, since 2010 ELECTRICAL PLANT RUSSIA) was used. This type of IM is used in mechanisms with a fan torque on the shaft: pumps, fans (with closed valves), etc. The following initial data were selected:  $\cos\phi_G=0.8$ ;  $\cos\phi_H=0.8$ ;  $K_\mu=1.5$ ;  $\cos\phi_D=0.8$ ;  $\cos\phi_{start}=0.45$ ;  $C=240$   $\mu$ F.

Harmonic analysis of the stator current signals and the IM torque operating under conditions of low-quality power supply and the construction of the corresponding travel time curves are implemented in the Mathcad software product.

To study the heating process of induction machines, the method of equivalent thermal circuits was used. For the study, the HELL 4AM90L4U3 was chosen ( $P_H=2.2$  kW,  $U_{1H}=220$  V,  $\cos\phi_H=0.83$ ,  $\eta_H=0.80$ ,  $s_H=0.051$ ). For the specified electric motor, the parameters of the equivalent cir-

cuit are:  $R_1=4.150$   $\Omega$ ;  $R_2=4.150$   $\Omega$ ;  $x_1=3.218$   $\Omega$ ;  $x_2=3.218$   $\Omega$ ;  $x_\mu=92.03$  Ohm. Thermal conductivities for an induction electric motor of the basic version 4AM90L4Y3 were:  $\Lambda_{13}=10.5707$  W/ $^\circ$ C;  $\Lambda_{23}=2.7648$  W/ $^\circ$ C;  $\Lambda_3=13.9969$  W/ $^\circ$ C; heat capacity:  $C_1=726.1$  J/ $^\circ$ C;  $C_2=3,260$  J/ $^\circ$ C;  $C_3=9,623$  J/ $^\circ$ C,  $\varepsilon_H=1$  bh/h;  $B=10,200$  K;  $\theta_{1H}=403$  K. An experiment was carried out to determine the heating curve of an IM of the 4AM90L4U3 type when operating with a rated load from a symmetrical supply voltage system.

For a generalized theoretical study of asymmetric induction machines, the experiment planning method was used, which makes it possible to assess the influence of the asymmetry of the stator electrical circuit on the operation of induction machines. The method of fractional factorial experiment was used in the work. The experiments were carried out on the basis of the design of a fractional factorial experiment of type 2<sup>6</sup>-1, taking into account star points. In the case of such an experiment with six factors, the number of experiments is reduced in comparison with a full factorial experiment. Additional experiments in the center of the design were used to obtain more accurate regression equations. The following factors were chosen as investigated: the coefficient taking into account the asymmetry in the electrical circuit of the AH stator phase –  $\varepsilon_A$  (dimensionless value), the coefficient taking into account the asymmetry in the electrical circuit of the IG stator phase B –  $\varepsilon_B$  (dimensionless), the coefficient taking into account the asymmetry in the electrical of the phase A circuit of the IM stator –  $\varepsilon_{dA}$  (dimensionless value) and the coefficient taking into account the asymmetry in the electrical circuit of the phase B of the IM stator –  $\varepsilon_{dB}$  (dimensionless value). The output parameters were taken:  $T$  – temperature rise of the stator winding IM ( $^\circ$ C); K2U – voltage unbalance factor (%). The levels of variation were set in such a way that the upper and lower limits corresponded to the boundaries of self-excitation of the IG. The experimental data were statistically processed using the Statistica and Statgraphics Centurion software applications.

---

#### 5. Results of research of processes in an induction motor when powered by an induction generator

---

##### 5.1. Mathematical model of an autonomous induction generator with capacitor excitation, taking into account losses in steel

The mathematical model of the IG is developed on the basis of the well-known equations of an induction machine in a three-phase coordinate system in matrix form and has the form [24, 25]:

$$\begin{aligned} d[\Psi_s]/dt &= [u_s] - [R_s][i_s]; \dots \\ d[\Psi_r]/dt &= [u_r] - [R_r][i_r] + j\omega[\Psi_r], \end{aligned} \quad (1)$$

where  $[u_s]=[u_A u_B u_C]^T$ ,  $[u_r]=[u_a u_b u_c]^T$  – transposed matrices of instantaneous values of stator and rotor phase voltages, respectively;  $[i_s]=[i_A i_B i_C]^T$ ,  $[i_r]=[i_a i_b i_c]^T$  – transposed matrices of instantaneous values of currents in the stator and rotor phases, respectively;  $[\Psi_s]=[\Psi_A \Psi_B \Psi_C]^T$ ,  $[\Psi_r]=[\Psi_a \Psi_b \Psi_c]^T$  – transposed matrices of full flux linkages of phase windings of the stator and rotor, respectively;

$$[R_s] = \begin{bmatrix} R_s & 0 & 0 \\ 0 & R_s & 0 \\ 0 & 0 & R_s \end{bmatrix}$$

– matrix of active resistances of stator windings;

$$[R_r] = \begin{bmatrix} R_r & 0 & 0 \\ 0 & R_r & 0 \\ 0 & 0 & R_r \end{bmatrix}$$

– matrix of active resistances of rotor windings;  $\omega$  – electrical frequency of rotation of the IG rotor.

Allowance for the saturation of the IG magnetic circuit is represented by the dependence of the mutual inductance  $L_\mu$  on the magnetizing current  $i_\mu$  [6]:

$$L_\mu = 1 / (a + b i_\mu^2), \tag{2}$$

where  $a, b$  – the coefficients of approximation of the magnetization curve.

For the IG excitation mode, capacitors are included in the stator circuit, therefore, in (1)

$$[u_s] = (-1/C) \int_0^t [i] dt + [u_0], \tag{3}$$

where  $[i] = [i_{cA} \ i_{cB} \ i_{cC}]^T$  – transposed matrix of instantaneous values of the currents that flow in the containers;  $[u_0] = [u_{0A} \ u_{0B} \ u_{0C}]^T$  – transposed matrix of instantaneous values of phase voltages at the initial moment of time  $t=t_0$ ;  $C$  – capacitance of the excitation capacitors.

The equation of motion of the IG has the form [6]

$$d\omega_g / dt = (M_{kr} - M_g) / J, \tag{4}$$

where  $\omega_g$  – mechanical rotation frequency of the IG (determines the electrical frequency of rotation of the rotor  $\omega = p\omega_g$ , where  $p$  – the number of pole pairs);  $J$  – the moment of inertia of the IG;  $M_g$  – electromagnetic moment of the IG;  $M_{kr}$  – the torque of an external source of mechanical energy.

In the case of an asymmetric system of exciting capacitors IG or load, the equations of electrical equilibrium for the stator phases will take the form:

$$[u'_s] = (-1/C) \int_0^t [i] dt + [u'_0], \tag{5}$$

where  $[u'_s] = [u'_A \ u'_B \ u'_C]^T$  – transposed matrix of instantaneous voltage values between the corresponding phase of the IG stator and the neutral of the load;  $[u'_0] = [u'_{0A} \ u'_{0B} \ u'_{0C}]^T$  – transposed matrix of instantaneous voltage values between IG neutrals and load.

Taking into account the complete internal symmetry of the machine and the balance of the system of currents ( $i_A + i_B + i_C = 0$ ), it can be argued that

$$u'_0 = (u'_{0A} + u'_{0B} + u'_{0C}) / 3. \tag{6}$$

The mathematical description for IM is compiled in the same way as for hypertension. The block diagram of the IG capacitive excitation system-IM is shown in Fig. 1.

To simplify the calculations of the characteristics of the IG-IM system with parametric asymmetry, an artificial technique is used: to take into account the asymmetry in the electrical circuit of the IM and IG stator, a dimensionless coefficient is introduced:

$$R'_{sA} = R_{sA} \cdot \epsilon_A, \quad R'_{sB} = R_{sB} \cdot \epsilon_B, \quad L'_{1A} = L_{1A} \cdot \epsilon_A^2,$$

$$L'_{1B} = L_{1B} \cdot \epsilon_B^2, \quad R'_{sdA} = R_{sdA} \cdot \epsilon_{dA}, \quad R'_{sdB} = R_{sdB} \cdot \epsilon_{dB},$$

$$L'_{1dA} = L_{1dA} \cdot \epsilon_{dA}^2, \quad L'_{1dB} = L_{1dB} \cdot \epsilon_{dB}^2, \tag{7}$$

where  $R_{sA}$  and  $R_{sB}$  – active resistances of phases A and B of the IG stator,  $R_{sdA}$  и  $R_{sdB}$  – active resistances of phases A and B of the IM stator,  $L_{1A}$  и  $L_{1B}$  – dissipation inductances of phases A and B of the IG stator,  $L_{1dA}$  and  $L_{1dB}$  – dissipation inductances of phases A and B of the IM stator,  $\epsilon$  – coefficient that takes into account the asymmetry in the electrical circuit of the stator of induction machines.

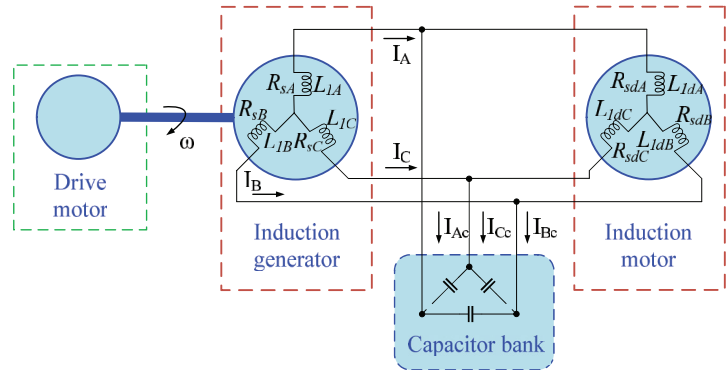


Fig. 1. Block diagram of the IG-capacitive excitation system-IM system

The existing IM models do not take into account the fact that the change in the magnetic flux (inductance) lags behind the change in the magnetizing current due to the properties of the domain structure of ferromagnets [26–28]. This property can be taken into account by shifting the magnetic flux signal with respect to the magnetizing current signal by the value of the angle  $\delta$  of the magnetic retardation (the angle of magnetic losses).

Finding the instantaneous value of the angle  $\delta$  of the magnetic lag is associated with difficulties in determining the instantaneous value of losses in steel in the high saturation mode of the IG magnetic circuit. Therefore, to determine the angle  $\delta$  at each integration step, let's use the following relation [29–31]:

$$\delta = \arctg \left( \frac{P_c}{P_{em.rms}} \right), \tag{8}$$

where  $P_c$  – value of losses in the stator steel at the current integration step;

$P_{em.rms}$  – effective value of electromagnetic power, which is found at each step of integration;

$$P_{em.rms} = \sqrt{\frac{1}{T} \int_0^T P_{em}^2 dt},$$

$$P_{em} = T_e \cdot \omega_r. \tag{9}$$

In [26], a dependence was substantiated for determining losses in steel, taking into account the nonlinear dynamics of domain structures and the unevenness of their motion at different magnetization reversal cycles, which ensures a high convergence of the calculated and experimental data:

$$P_c(I_\mu) = \frac{\xi}{dE(I_\mu)/dI_\mu} (E(I_\mu))^2, \tag{10}$$

where  $I_\mu$  – effective value of the magnetizing current;  $\xi$  – coefficient depending on the characteristics of electrical steel;  $E(I_\mu)$  – dependence of the EMF on the magnetizing current.

Thus, expressions (1)–(10) form a mathematical model of IM in a three-phase coordinate system, which takes into account the inertia of the magnetization process, which manifests itself in the time and phase lag of the magnetization with respect to the magnetic field strength.

The block diagram of the IG mathematical model with allowance for losses in steel is shown in Fig. 2.

The influence of the asymmetry of the IG output voltage on the dynamic mechanical characteristics of the IM is expressed by an increase in the amplitude of the oscillations of the dynamic electromagnetic moment. This negatively affects the operation of both the electric motor and the mechanical part of the electric drive.

Lowering the voltage at the output of the IG leads to the value of the asymmetry coefficient, calculated by the expression:

$$U_1 = \sqrt{\frac{1}{12} \left( \left( \sqrt{3} \cdot U_{AB} + \sqrt{4 \cdot U_{BC}^2 - \left( \frac{U_{BC}^2 - U_{CA}^2}{U_{AB}} + U_{AB} \right)^2} \right)^2 \right) + \left( \frac{U_{BC}^2 - U_{CA}^2}{U_{AB}} \right)^2},$$

$$U_2 = \sqrt{\frac{1}{12} \left( \left( \sqrt{3} \cdot U_{AB} - \sqrt{4 \cdot U_{BC}^2 - \left( \frac{U_{BC}^2 - U_{CA}^2}{U_{AB}} + U_{AB} \right)^2} \right)^2 \right) + \left( \frac{U_{BC}^2 - U_{CA}^2}{U_{AB}} \right)^2},$$

$$K_{2U} = \frac{U_2}{U_1} \cdot 100, \tag{11}$$

where  $U_1$  – positive sequence voltage of the fundamental frequency;  $U_2$  – negative sequence voltage of the fundamental frequency;  $K_{2U}$  – voltage unbalance factor.

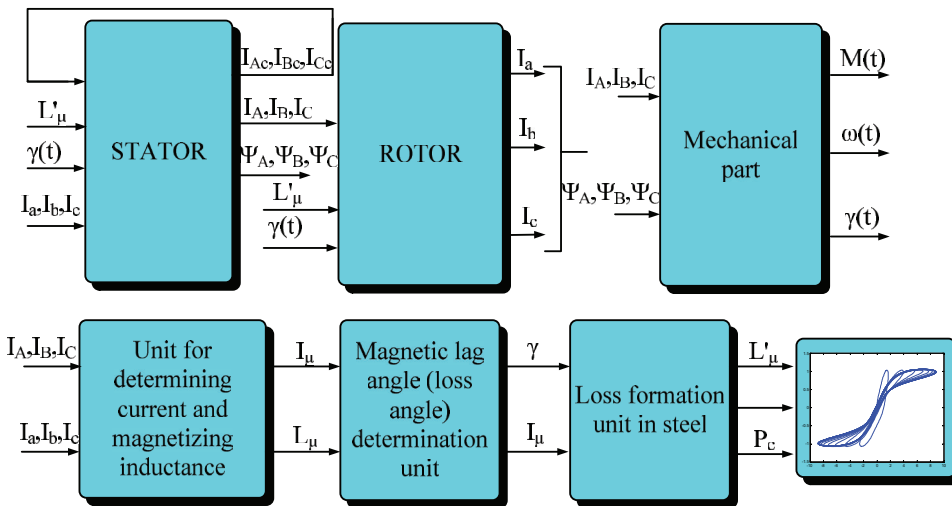


Fig. 2. Block diagram of the mathematical model of an induction generator taking into account losses in steel

### 5.2. Results of modeling the start of an induction motor from an autonomous induction generator with parametric asymmetry

Using the developed mathematical model, an analysis of the characteristics of an IG operating at a high saturation of the magnetic system is carried out.

Fig. 3 shows the obtained dynamic hysteresis loops.

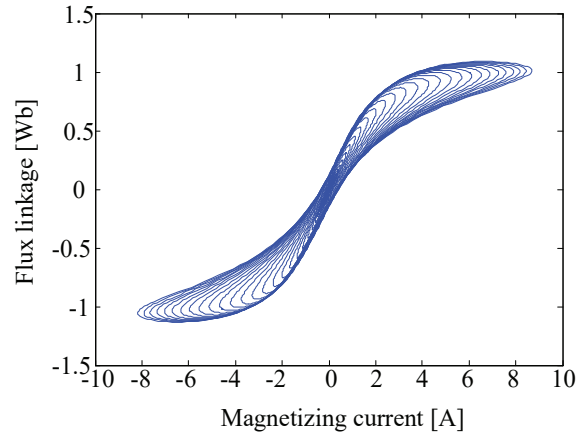


Fig. 3. Calculated hysteresis loops during self-excitation of an autonomous induction generator

Using the IG model under load, a study of the operation of a generator with a rated power of a motor mode of 2.2 kW with excitation from capacitor banks and an IM with a power of 1.3 kW was carried out.

Studies have shown that when the excitation capacitance of the IG is less than 80 μF per phase, when the capacitors are connected to a star, the rotation speed of the IM does not reach the nominal value. This is due to the fact that an increase in the active current in the generator network when starting the IM leads to demagnetization of the generator and a sharp decrease in the network voltage to zero. With an increase in the capacity, the start of the IM becomes possible, while the larger the excitation capacity, the less time it takes to start. The oscillogram of the voltage and current from the generator network at the start of the IM, obtained during the simulation, is shown in Fig. 4.

Autonomous power systems contain induction electric motors as drives for various mechanisms. Therefore, the requirements for starting induction squirrel-cage motors of comparable power are imposed on the generator complex, which provides power supply to autonomous systems. When the induction motor is turned on, the switching devices of the electric unit or power plant should not turn off.

When using generating sets in electrical power take-off installations from the car engine, it is required to start the electric motors of 50 % of the power.

To determine the overload capacity of the IG, taking into account the parametric asymmetry, the possibility of direct starting of the IM from the IG with capacitor excitation is considered. With a stationary rotor, the IM represents a small active-inductive resistance for the power grid, deter-

mined by the active resistances and leakage inductances of the stator and rotor circuits. The impedance of the motor in short-circuit mode (with a stationary rotor) determines the multiplicity of the motor starting current in relation to the nominal one. Therefore, knowing the nominal ( $\phi_n$ ) and starting ( $\phi_{start}$ ) phase displacement angles between the current and voltage of the induction motor, it is possible to determine the active and reactive conductivity of the motor at the moment of its connection to the network.

For a general industrial IM, during start-up up to critical slip,  $\sin\phi_{start}$  is close to unity, while  $\sin\phi_{start}=0.4...0.5$ . Thus, during the start-up process, the engine is a large inductive load and loads the autonomous generator with reactive power.

For IG, this power is demagnetizing and must be compensated for by the capacitive reactive power of the excitation capacitors. If the capacitance of the capacitors is not enough, then the generator is de-excited for two or three periods of current.

To maintain the IG self-excitation mode, a balance of active and reactive powers of the generator and load is required.

According to [4], the algebraic sum of the reactive powers of the autonomous system IG – the load is equal to:

$$\sum_{k=1}^n Q_k = 0.$$

In the general case, the reactive power of the capacitor banks is equal to the sum of the reactive powers of the generator and the load:

$$Q_c = \frac{U^2}{x_c} = Q_g + Q_n = P_g \cdot \text{tg}\phi_g + P_n \cdot \text{tg}\phi_n, \tag{12}$$

where  $U_c$  – linear voltage module at the terminals of the capacitor bank, which is determined by the voltage at the IG terminals ( $U_c=U_g$ );  $P_g, P_n$  – rated active power of the generator and its load.

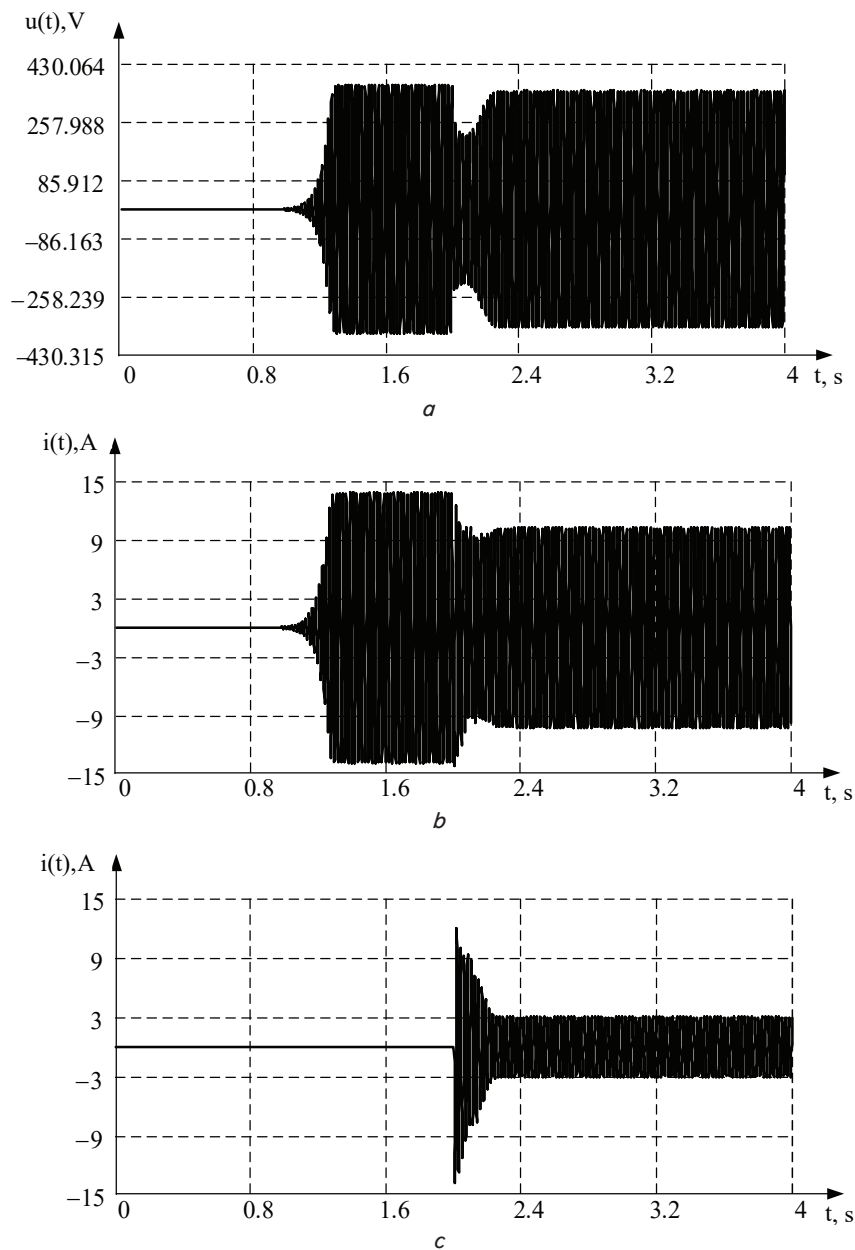


Fig. 4. Curves of voltage: *a* – stator current of an induction generator; *b* – and the stator current of the induction generator; *c* – at start-up

From equation (12) it can be seen that the number of capacitors is mainly determined by the power factor of the load, which must be provided by the induction generator complex.

For real loads of autonomous objects  $\cos\phi_n$  lies in the range of 0.6...1.0. As studies have shown, with such a nominal load power factor in the process of starting the electric motor in the power system, first of all, the balance of reactive power of the generator and the engine is disturbed. Thus, the maximum power of the motors started from the IG is determined from the equation for the balance of reactive conductivity:

$$P_M = \frac{\left(\frac{U_c}{K_\mu}\right)^2 \cdot \omega_0 \cdot C - P_g \cdot \text{tg}\phi_g}{\text{tg}\phi_{start}}, \quad (13)$$

where  $\omega_0 = 2\pi f_c$  – cyclic frequency of voltage fluctuations in the stator winding,  $K_\mu$  – coefficient that takes into account the reduction in the consumption of reactive current by the generator during a voltage drop during the start of the IM,  $C_{max}$  – maximum value of the capacitance connected to the IG.

Fig. 5 shows a graph of the required power of the induction generator depending on the power of the connected motor under various operating modes.

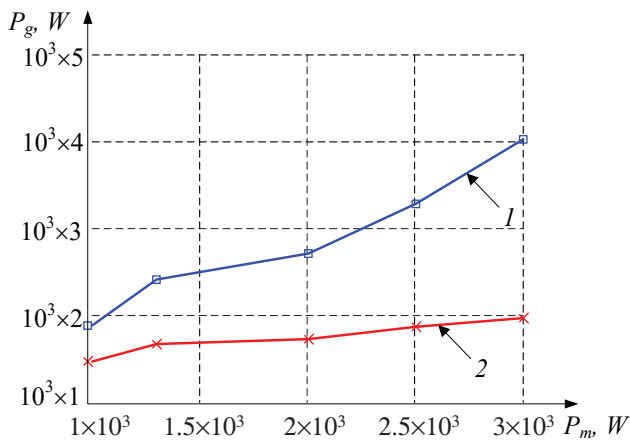


Fig. 5. The required power of the induction generator, depending on the power of the connected motor under various operating modes (excitation capacity – 240 μF): 1 – during start; 2 – steady state

For real values of the parameters of induction machines of various designs, the value of the ratio of the power of the started engine and the generator lies within:

$$p = \frac{P_M}{P_G} \approx 0.5 \div 0.7.$$

Also, the parametric asymmetry in the stator windings of the IM also affects the value of the required power of the IG.

In Fig. 6, using equation (13), graphs of the required power of the IG are presented for various types of parametric asymmetry in the windings of induction machines.

The ideal three-phase voltage was first used as a power supply, and then - power supply from the IG with parametric asymmetry.

Fig. 7 shows the obtained graphs of transient processes (start, surge in rated load) at ideal and distorted voltage.

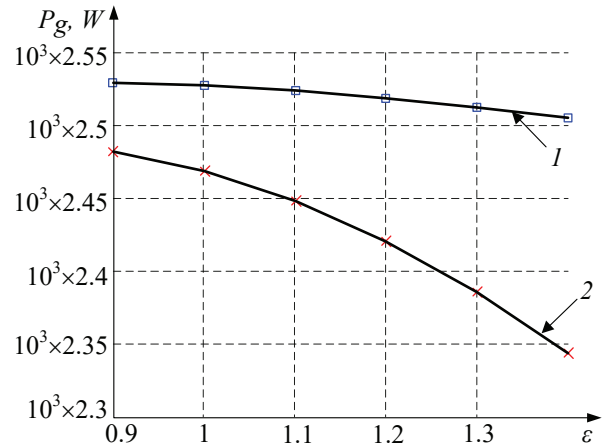


Fig. 6. The required power of the induction generator, depending on the unbalance factor for: 1 – during start; 2 – steady state

The presence of harmonic components in the IM supply leads, as can be seen, to the occurrence of torque pulsations (7–10 %).

The hodograph of the IM moment during one revolution has the form shown in Fig. 8.

The instantaneous values of the IM stator currents obtained in the considered example in the steady state have the form shown in Fig. 9.

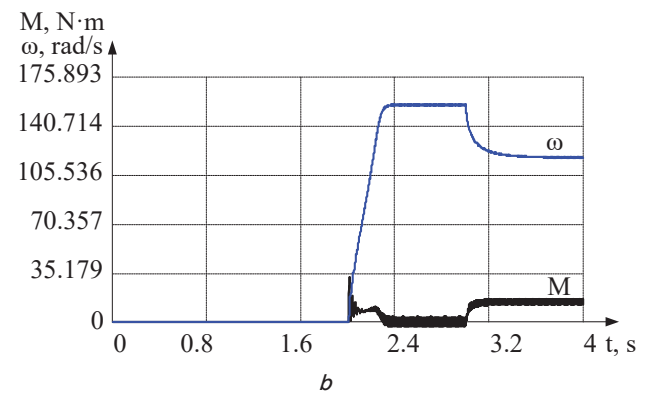
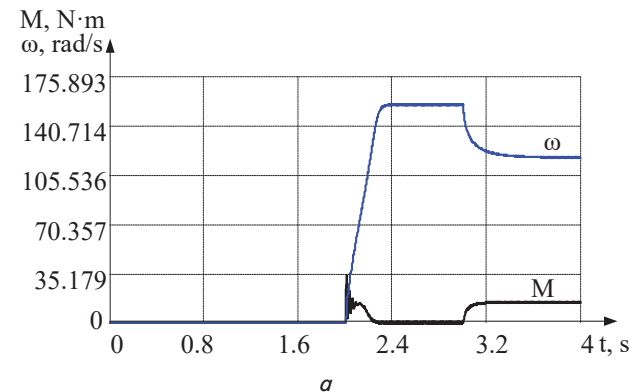


Fig. 7. Torque and speed of the induction generator at start and load surge: a – when ideal power supply; b – when powered by an induction generator with parametric asymmetry

In accordance with the graphs, due to the asymmetry of the output voltage, the amplitude of the oscillations of the electromagnetic moment increases by 18 %. With an unbalance ratio of 3.72 %, the stator phase A current increased by 23 %.

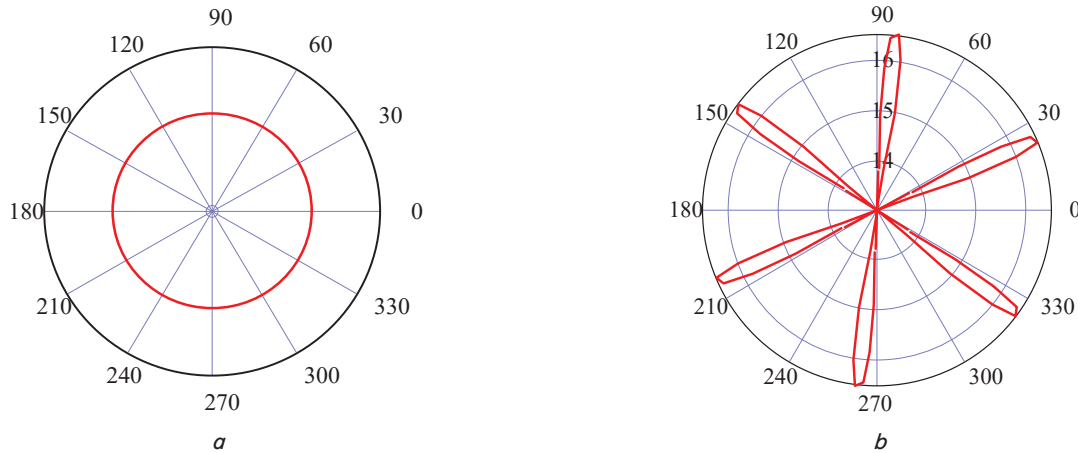


Fig. 8. Hodograph of the moment of the induction generator: *a* – when ideal power supply; *b* – when powered by an induction generator with parametric asymmetry

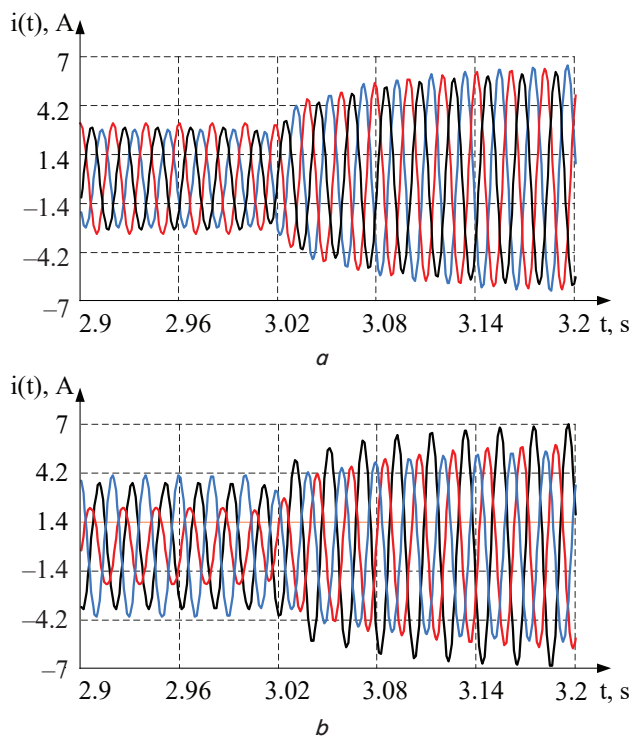


Fig. 9. Stator currents of an induction generator: *a* – when ideal power supply; *b* – when powered by an induction generator with parametric asymmetry

**5. 3. Development of a thermal model of the “induction generator-induction motor” system with asymmetry in the stator windings**

Analytical studies of the thermal state of an IM when powered by an autonomous IG with parametric asymmetry in the stator windings were carried out using an equivalent thermal circuit (ETC) [32–34]. Sufficiently accurate results in the study of thermal processes in induction machines can be obtained using a thermal model consisting of three bodies [35–37]. The first is the stator winding, the second is the stator steel and the frame, the third is the rotor [37]. The three-mass thermal substitution model is valid for self-ventilated induction machines. Therefore, to compile a thermal model, an equivalent thermal equivalent circuit was built. Shown in Fig. 10 the

thermal equivalent circuit of an induction motor is drawn up for this representation.

The system of differential equations describing the thermal state of the machine according to Fig. 10:

$$\left. \begin{aligned} C_1 \frac{d\tau_1}{dt} &= \Delta P_1 - \lambda_1 \tau_1 - \lambda_{12} (\tau_1 - \tau_2) - \lambda_{13} (\tau_1 - \tau_3); \\ C_2 \frac{d\tau_2}{dt} &= \Delta P_2 - \lambda_2 \tau_2 - \lambda_{12} (\tau_1 - \tau_2) - \lambda_{23} (\tau_3 - \tau_2); \\ C_3 \frac{d\tau_3}{dt} &= \Delta P_3 - \lambda_3 \tau_3 - \lambda_{23} (\tau_3 - \tau_2) - \lambda_{31} (\tau_3 - \tau_1). \end{aligned} \right\} \quad (14)$$

The notation in the system of equations is as follows:

- $\tau_1, \tau_2, \tau_3$  – temperature rise of the stator, steel and rotor windings above the ambient temperature;
- $\Delta P_1, \Delta P_2, \Delta P_3$  – heat output;
- $C_1, C_2, C_3$  – heat capacity of bodies;
- $\lambda_1, \lambda_2, \lambda_3$  – thermal conductivity from the stator, steel and rotor windings into the environment;
- $\lambda_{12}, \lambda_{13}, \lambda_{23}$  – thermal conductivity between bodies.

The active power losses in the stator and rotor windings were determined according to [38–40]. The magnetic losses caused by the phenomenon of hysteresis and eddy currents in the stator core were estimated according to expression (10).

The results of calculating the temperature rises of the winding, rotor and steel of an induction electric motor 4AM90L4U3 as a function of time at rated load are shown in Fig. 10.

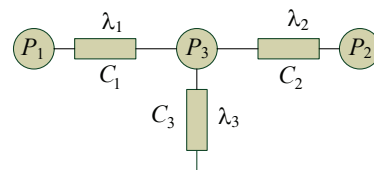


Fig. 10. Three-mass thermal replacement model of an induction motor

It is found that the motor of the AOL2-31-4 type reaches the steady-state value of the overheating temperature of the stator winding 90...100 minutes. To determine the value of the overheating temperature with an asymmetry of the supply voltage, let’s take the setting of a practically heated state of 95 minutes.

Research has been carried out on heating the stator winding of an IM with a rated load with an asymmetry of the supply voltage  $K_{2U}=0.94\%$  and  $K_{2U}=4.04\%$ .

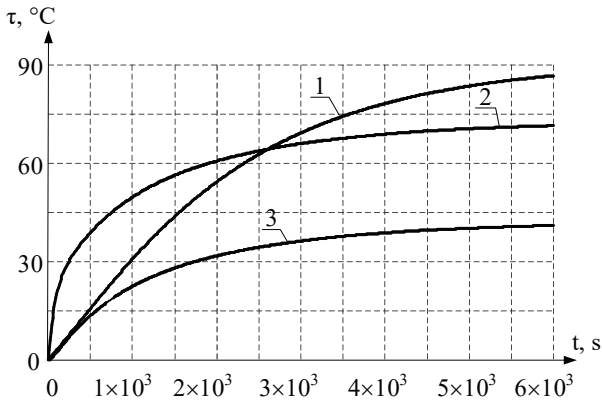


Fig. 11. Heating curve of the windings of an induction motor of type 4AM90L4U3 in nominal conditions: 1 – stator; 2 – rotor, 3 – steel

From Fig. 12, 13 it is possible to see that the shape of the heating curves of the stator winding and the IM steel depends on  $\epsilon$ . With an increase in the coefficient  $\epsilon$ , there is an increase in the asymmetry coefficient, the rate of rise of the winding temperature and the temperature of the steel, the values of which may exceed the maximum permissible values [41–44].

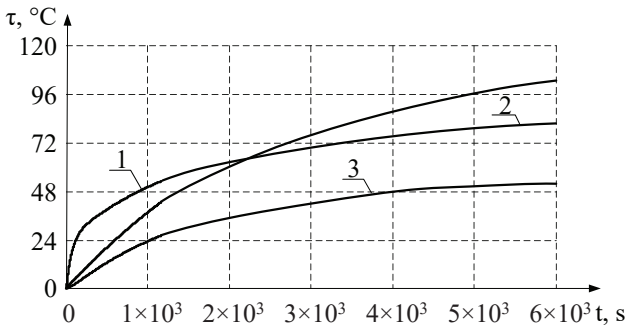


Fig. 12. Heating curves  $\tau_1=f(t)$ ,  $\tau_2=f(t)$  and  $\tau_3=f(t)$  at  $K_{2U}=0.94\%$  ( $\epsilon=0.8$ ) for the 4AM90L4U3 electric motor

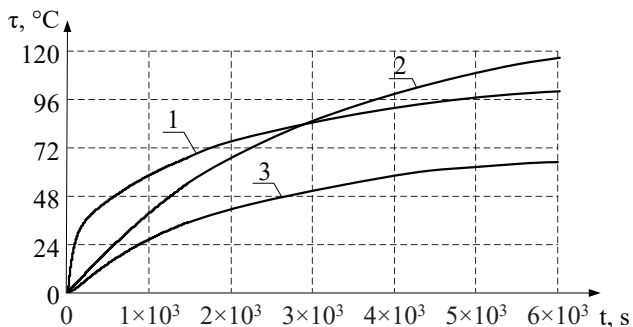


Fig. 13. Heating curves  $\tau_1=f(t)$ ,  $\tau_2=f(t)$  and  $\tau_3=f(t)$  at  $K_{2U}=4.04\%$  ( $\epsilon=1.6$ ) for the 4AM90L4U3 electric motor

The comparison of the results of the experimental determination of the average temperature rise with the analytical calculation is done (Table 1). For this, according to the

previously described method, the overheating of the stator winding of the IM is determined, taking into account the presence of parametric asymmetry in the stator windings of the IG and IM.

Table 1

Comparison of the results of an experimental and analytical study of the influence of supply voltage asymmetry on the average temperature rise of the stator winding of a 4AM90L4U3 motor

No.	$K_{2U}, \%$	$T_{exp}, ^\circ\text{C}$	$T_{dif}, ^\circ\text{C}$	Error, %
1	0	83,47	82,1	1,64
2	0,91	85,52	86,92	1,637
3	3,732	98,13	93,69	4,52
4	9,12	211,97	221,33	4,41

**5. 4. Development of a regression model of the “induction generator-induction motor” system with asymmetry in the stator windings**

To study the factors affecting thermal processes and the quality of electricity in the “induction generator-induction motor” system with asymmetry in the stator windings, the theory of experiment planning was used. The use of experimental planning methods allows one to obtain the necessary regression model of the process under study [45–47]. Due to the large number of variable factors, the use of a full factorial experiment (FFE) will lead to a large number of necessary experiments. It is possible to reduce their number without significant loss of significant information about the process under study by using a fractional factorial experiment (FrFE). It is advisable to use FrFE with the number of factors from three or more, if for economic or any other reasons it is unprofitable to produce.

The fractional rotatable compositional plan consists of three parts: the core of the FrFE  $2^{k-p}$  design (here  $k$  – the number of factors,  $p$  – the number of interactions of factors), “star” points with coordinates  $(\pm\alpha, 0, \dots, 0)$ ,  $(0, \pm\alpha, \dots, 0)$ , ...,  $(0, 0, \dots, \pm\alpha)$  by the number of  $2k$  and  $n$  points in the center of the plan with coordinates  $(0, 0, \dots, 0)$ .

Number of trials (with two trials in the center of the plan):

$$N_0 = 2^{k-1} + 2 \cdot k + 2 = 32 + 2 \cdot 6 + 2 = 46. \tag{15}$$

The matrix for planning a fractional factorial experiment of the type  $2^{k-1}$  and its results are presented in Table 2.

The significance of the model coefficients was determined using the  $p$ -level and is shown on standardized Pareto charts (Fig. 14). The standardized Pareto charts shown in Fig. 14, allow to establish significant factors. The intersection of the standardized effects with a vertical line, which represents the 95 % confidence level, means that the influence of factors on the response function is statically significant.

The greatest effect on the level of the voltage unbalance coefficient is exerted by the linear effects of the coefficients, which take into account the asymmetry in the electrical circuit of the IG stator and the quadratic interactions of the coefficients. In this case, the “plus” sign on the Pareto charts indicates an increase in the stress unbalance coefficient with an increase in the factor (Fig. 14, a).

Table 2

Planning matrix and experiment results

No.	$\epsilon_A$	$\epsilon_B$	$\epsilon_{dA}$	$\epsilon_{dB}$	$C_A$	$C_B$	$K_{2U}$	$T$
1	1.0	1.47568	1.0	1.0	300.0	300.0	2.182	83.49
2	0.8	0.8	1.2	0.8	320.0	280.0	1.098	87.13
3	1.2	1.2	0.8	1.2	320.0	280.0	3.732	80.72
4	0.8	0.8	0.8	1.2	320.0	280.0	0.3071	86.95
5	1.2	1.2	1.2	1.2	320.0	320.0	4.262	93.69
6	1.0	1.0	0.524317	1.0	300.0	300.0	0.5564	69.38
7	0.8	1.2	1.2	1.2	280.0	320.0	3.845	98.39
8	0.8	0.8	1.2	1.2	320.0	320.0	0.2597	101.4
9	0.8	0.8	1.2	0.8	280.0	320.0	0.1822	87.1
10	1.2	1.2	0.8	0.8	320.0	320.0	4.195	72.21
11	0.8	1.2	0.8	1.2	280.0	280.0	3.562	85.32
12	1.2	1.2	0.8	0.8	280.0	280.0	2.918	71.36
13	1.0	1.0	1.0	0.524317	300.0	300.0	2.31	69.91
14	1.2	0.8	1.2	0.8	280.0	280.0	4.33	84.83
15	1.2	1.2	1.2	0.8	320.0	280.0	5.032	82.01
16	1.2	0.8	0.8	0.8	280.0	320.0	3.578	74.51
17	1.2	1.2	1.2	0.8	280.0	320.0	3.408	82
18	1.2	0.8	0.8	1.2	320.0	320.0	4.444	84.3
19	1.2	0.8	0.8	0.8	320.0	280.0	5.137	75.54
20	1.0	1.0	1.0	1.0	300.0	252.432	1.723	84.82
21	0.8	1.2	1.2	0.8	320.0	320.0	2.23	85.31
22	0.8	0.8	0.8	0.8	320.0	320.0	0.3307	76.48
23	1.2	0.8	1.2	1.2	280.0	320.0	3.426	97.48
24	0.8	0.8	1.2	1.2	280.0	280.0	0.5632	101
25	1.0	1.0	1.0	1.0	300.0	300.0	1.435	84.57
26	1.0	1.0	1.0	1.47568	300.0	300.0	0.8714	96.66
27	1.0	1.0	1.0	1.0	347.568	300.0	2.774	84.92
28	1.0	1.0	1.0	1.0	300.0	347.568	1.355	84.9
29	0.8	1.2	1.2	0.8	280.0	280.0	2.457	84.96
30	0.8	1.2	0.8	0.8	280.0	320.0	3.519	74.9
31	1.2	1.2	1.2	1.2	280.0	280.0	2.912	93.09
32	1.2	0.8	1.2	0.8	320.0	320.0	5.608	85.31
33	1.2	0.8	0.8	1.2	280.0	280.0	3.168	84.17
34	0.8	0.8	0.8	0.8	280.0	280.0	0.4459	76.31
35	1.0	1.0	1.47568	1.0	300.0	300.0	1.909	97.25
36	0.8	1.2	0.8	0.8	320.0	280.0	2.024	74.19
37	1.2	0.8	1.2	1.2	320.0	280.0	5.021	98.03
38	1.0	1.0	1.0	1.0	252.432	300.0	0.534	84.8
39	0.524317	1.0	1.0	1.0	300.0	300.0	5.275	91.53
40	0.8	1.2	0.8	1.2	320.0	320.0	3.227	85.49
41	0.8	1.2	1.2	1.2	320.0	280.0	2.322	97.72
42	1.0	1.0	1.0	1.0	300.0	300.0	1.438	84.56
43	1.2	1.2	0.8	1.2	280.0	320.0	2.245	81.12
44	0.8	0.8	0.8	1.2	280.0	320.0	1.232	87.17
45	1.47568	1.0	1.0	1.0	300.0	300.0	6.906	83.06
46	1.0	0.524317	1.0	1.0	300.0	300.0	3.388	91.26

From the Pareto map for the excess of the temperature of the stator winding of the IM (Fig. 14, b), it can be seen that of the main components, the linear effects of the coefficients, taking into account the asymmetry in the electrical circuit of the stator of the IG and IM, turned out to be statistically significant. The rest of the factors turned out to be weakly significant.

After excluding statistically insignificant coefficients, mathematical models of the second order in natural form,

describing the dependence of the temperature rise of the IM stator winding ( $T$ ) and the voltage unbalance factor ( $K_{2U}$ ) on the coefficients that take into account the asymmetry in the electric circuit of the stator of induction machines, will take the form:

$$K_{2U} = 55.9345 - 47.1848\epsilon_A + 21.805\epsilon_A^2 - 19.3556\epsilon_A\epsilon_B + 0.120733\epsilon_A C_A + 7.1965\epsilon_B^2, \quad (16)$$

$$\begin{aligned}
 T = & 86.3239 - 16.8743\epsilon_A - 20.9334\epsilon_B + \\
 & + 26.3988\epsilon_{dA} + 36.9755\epsilon_{dB} + 12.5491\epsilon_A^2 - \\
 & - 8.36719\epsilon_A\epsilon_B - 2.88281\epsilon_A\epsilon_{dA} - \\
 & - 9.55469\epsilon_A\epsilon_{dB} + 12.9027\epsilon_B^2 - \\
 & - 3.89844\epsilon_B\epsilon_{dA} - 3.66406\epsilon_B\epsilon_{dB} - \\
 & - 5.04\epsilon_{dA}^2 - 5.17259\epsilon_{dB}^2.
 \end{aligned}
 \tag{17}$$

The performance of the model is confirmed by a high coefficient of determination  $R^2$ , equal to 90.47 % for the volt-

age unbalance coefficient and 99.93 % for the temperature rise of the IM stator winding.

Fig. 15 shows the response surfaces of the dependent variable – the voltage unbalance coefficient and the temperature rise of the stator winding of an induction motor depending on the most significant factors (with fixed values of the remaining factors) for natural designations of factors. The graphs in Fig. 15 one of the factors fixes and changes the values of the other two factors, therefore, the response surfaces allow one to see not only the influence of an individual factor on the output value, but also their paired interaction.

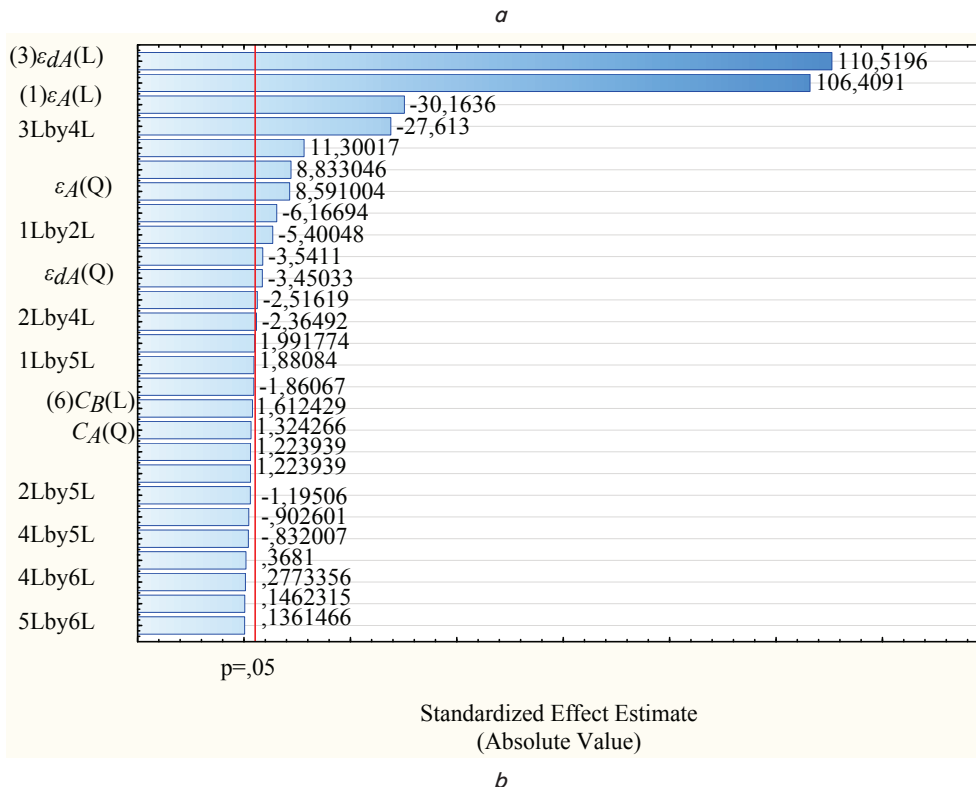
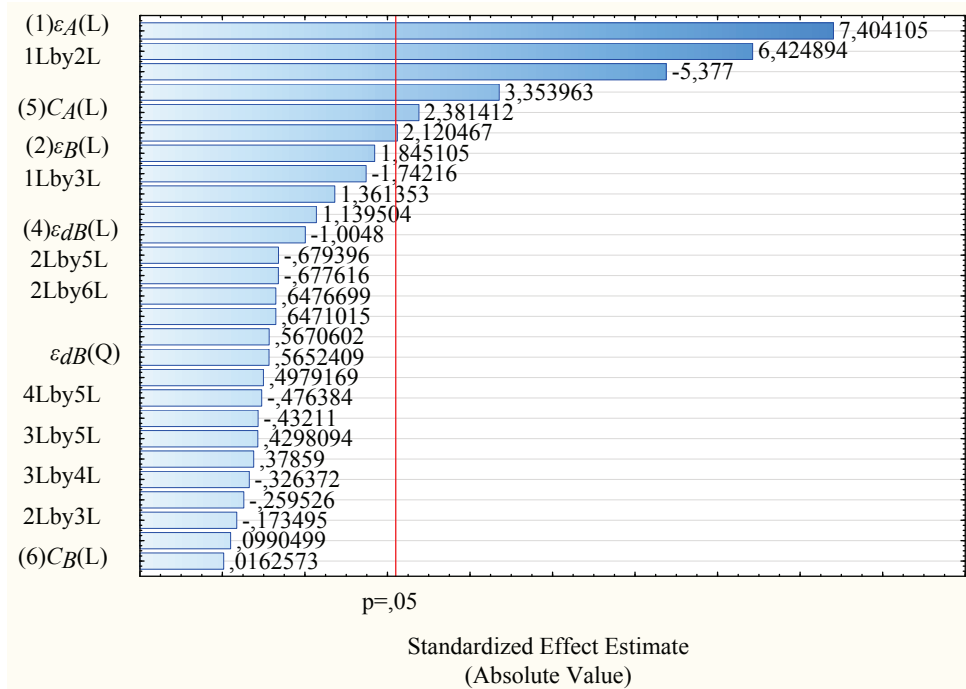


Fig. 14. Pareto chart: *a* – for voltage unbalance coefficient; *b* – for power consumption

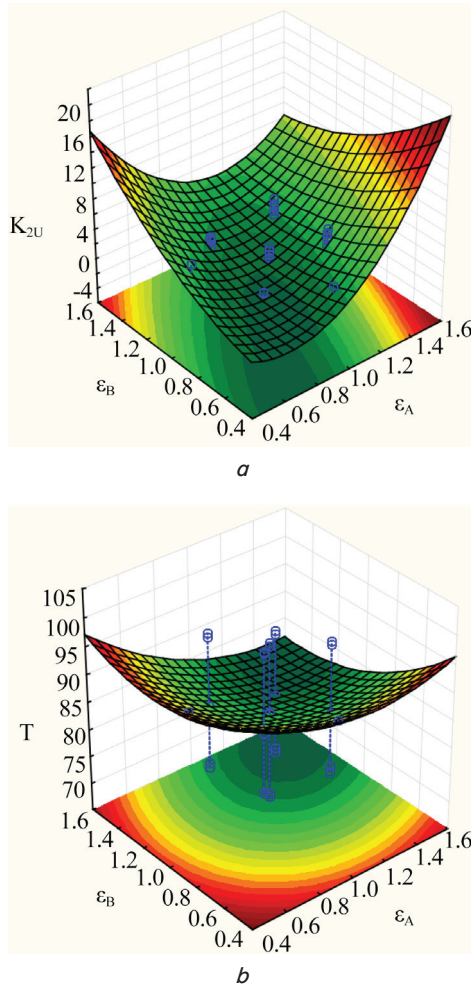


Fig. 15. Response surface: *a* – characterizing the dependence of the voltage unbalance coefficient; *b* – temperature rise of the stator winding of the induction motor; on the coefficients that take into account the asymmetry in the electrical circuit of the stator of an induction generator

The response surface shown in Fig. 15, *a*, indicates a significant difference in the dependence of the asymmetry coefficient on the coefficient taking into account the asymmetry in the electrical circuit of phases *A* and *B* of the IG stator. The intensity of the change in the asymmetry coefficient from the coefficient taking into account the asymmetry in the electrical circuit of phase *A* is greater than from the change in the coefficient taking into account the asymmetry in the electrical circuit of phase *B*.

Fig. 15, *b* shows the response surfaces of the dependence of the asymmetry coefficient on the coefficient taking into account the asymmetry in the electric circuit of phases *A* and *B* of the IG stator. A pronounced directly proportional dependence within the factor space shows that with an increase in the coefficient taking into account the asymmetry in the electrical circuit of phases *A* and *B* of the stator, the temperature of the windings decreases.

To find the influence of the rate of increase of significant factors on the response function, the partial derivatives of the obtained regression equations (16), (17) were determined and the corresponding depen-

dencies were constructed (Fig. 16–18). Partial differential equations are required when the described behavior of the system is a function of more than one variable.

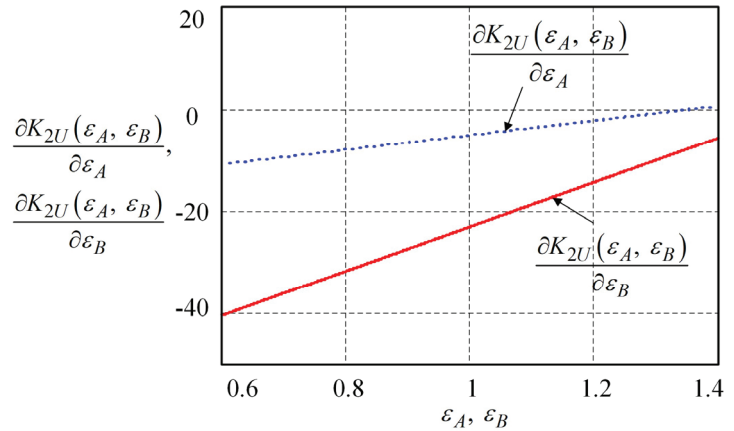


Fig. 16. Dependence of the rate of rise of the function of the voltage unbalance coefficient on the coefficients that take into account the unbalance in the electrical circuit of phases *A* and *B* of the stator of an induction generator

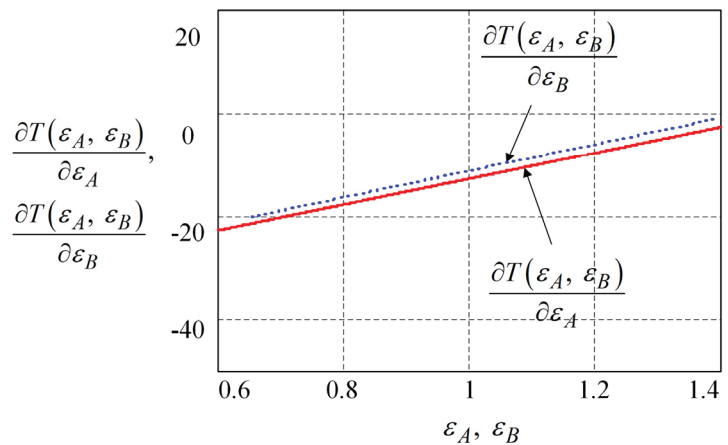


Fig. 17. Dependence of the rate of rise of the function of the temperature rise of the stator winding of an induction motor on the coefficients that take into account the asymmetry in the electrical circuit of phases *A* and *B* of the stator of the induction generator

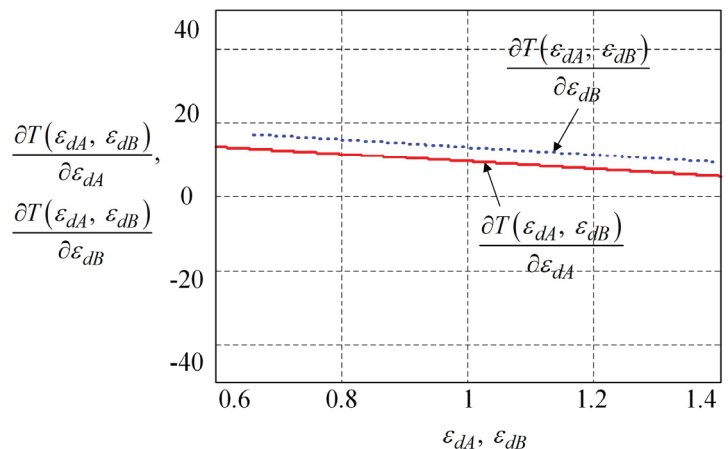


Fig. 18. Dependence of the slew rate of the function of the temperature rise of the stator winding of an induction motor on the coefficients that take into account the asymmetry in the electrical circuit of phases *A* and *B* of the stator of an induction motor

## 6. Discussion of the results of the study of processes in an induction motor when powered by an induction generator

From Fig. 5 it follows that an increase in the asymmetry factor in the steady state is a significant decrease in the power of the IG, which is necessary to supply the IM. In this case, the amount of generator power required to start the engine practically does not depend on the asymmetry of the stator windings. Based on the study of the operation of the IG on the network with a motor load, it can be argued that in the IG network, with an increase in the capacity of the capacitors, it is possible to start an induction motor with a power of not more than 60 % of the generator power. This conclusion was also confirmed in the course of the experiment.

Calculations made on the basis of an induction machine type AOLS2-21-4 with the following parameters:  $\cos\varphi_G=0.8$ ;  $\cos\varphi_H=0.8$ ;  $K_\mu=1.5$ ;  $\cos\varphi_D=0.8$ ;  $\cos\varphi_{start}=0.45$ ,  $C=240 \mu\text{F}$ , gave the value of the required power of the induction generator  $P_r=2.22 \text{ kW}$  at start and  $P_r=1.67 \text{ kW}$  when operating in a steady state. The practical significance of the results obtained lies in the possibility of wide application of the results obtained for the complex solution of the problems of reliable and efficient autonomous power supply of agricultural consumers.

Taking into account the results of the study and the characteristics of agricultural consumers and their modes of operation, an induction generator can be recommended as a source of electrical energy in autonomous power supply systems.

The analysis of the obtained characteristics of the IM operation showed that the poor quality of the IG output voltage causes an increase in the stator current, and, accordingly, an increase in losses and a decrease in the efficiency of the motor. In this case, there is an increase in "heating" losses due to poor quality of the supply voltage, which is determined, as is known, by the state of the motor and the power supply.

Analysis of the dependencies shown in Fig. 12, 13 shows that the heating rates of the electric motor units at the initial heating moment differ significantly. So, the heating rate of steel at the initial moment significantly lags behind the heating rate of the winding. Studies have shown that the asymmetry of the output voltage of an induction generator can reach 3–10 % (which is higher than the permissible 2 %) and causes overheating of the stator windings in excess of the maximum permissible values.

As follows from the Table 1, the error between the results of the experimental and analytical studies does not exceed 5 %. Thus, it is possible to draw a conclusion about the adequacy of the proposed methodology for determining the effect of reducing the quality indicators of the supplying electricity using a generalized thermal model.

The developed mathematical model of the thermal state of the IG-IM system differs from the existing models by taking into account the quality of the supply energy from the point of view of thermal processes. This makes it possible to estimate the real heating of the stator winding insulation and, accordingly, the real life of its service. The influence on the heating of the phase windings of the stator of the IM and the quality of the generated voltage is determined not only by deviations from the passport parameters of the motor itself, but also by the power source, in particular IG with capacitor excitation.

The analysis of the response surfaces showed that with an increase in the coefficient taking into account the asym-

metry in the electric circuit of the stator phases in the steady state, there is a decrease in the temperature of the stator windings, which must be taken into account when designing generating systems based on IG. A change in the parameters of the unbalance of the stator of induction machines can cause a large voltage drop in the generator, a decrease in the stability of the IM operation, and, therefore, lead to demagnetization of the IG when starting motors of relatively high power.

Analysis of Fig. 16 shows that the rate of change of the voltage unbalance coefficient depends more on the coefficient that takes into account the unbalance in the electrical circuit of phase *B* than on the coefficient that takes into account the unbalance in the electrical circuit of phase *A*, the greatest influence is exerted by the parametric asymmetry of the *B* phase of IG. In this case, with an increase in the values of the coefficients taking into account the asymmetry in the electrical circuit, their influence becomes comparable.

The partial derivatives  $\frac{\partial K_{2U}}{\partial \varepsilon_A(\varepsilon_B)}$ ,  $\frac{\partial T}{\partial \varepsilon_A(\varepsilon_B)}$  and  $\frac{\partial T}{\partial \varepsilon_A(\varepsilon_B)}$  relative to  $\varepsilon_A$  and  $\varepsilon_B$ , respectively, show the rate at which the temperature rise of the IM stator winding changes, if the coefficient taking into account the asymmetry in the electrical circuit of the phases *A* and *B* of the IG stator, respectively, changes, and the remaining coefficients remain unchanged. Similarly for  $\frac{\partial T}{\partial \varepsilon_{dB}}$  and  $\frac{\partial T}{\partial \varepsilon_{dA}}$ .

From Fig. 17 it is possible to see that the graph of dependence  $\frac{\partial T}{\partial \varepsilon_{dB}}$  on  $\varepsilon_B$  is slightly higher than the graph of dependence  $\frac{\partial T}{\partial \varepsilon_A}$  on  $\varepsilon_A$ , this means that the speed, with a change in the temperature rise of the stator winding of the IM, is more strongly influenced by the coefficient that takes into account the asymmetry in the electrical circuit of the phase *B* of the IG stator –  $\varepsilon_{dB}$  than the coefficient that takes into account the asymmetry in the electrical circuit of the phase *A* of the stator IG –  $\varepsilon_{dA}$ .

Similarly, from Fig. 18 it is possible to see that the graph (or straight line) of dependence  $\frac{\partial T}{\partial \varepsilon_{dB}}$  on  $\varepsilon_{dB}$  is slightly higher than the graph of dependence on  $\varepsilon_{dA}$ , which means that the rate of change in the temperature rise of the IM stator winding is more influenced by the coefficient that takes into account the asymmetry in the electrical circuit of phase *B* of the IM stator –  $\varepsilon_{dB}$  than the coefficient that takes into account asymmetry in the electrical circuit of the phase *A* of the stator of the IM –  $\varepsilon_{dA}$ .

The results obtained make it possible to determine the most significant factors that affect the temperature processes occurring in the IM when powered by the IG as part of an autonomous electric power plant used in agricultural activities. Equations (16), (17) can be used when carrying out a comprehensive assessment of the thermal state of the IM at various parameters of asymmetry in the stator windings.

Despite its versatility, the method also has significant limitations. The resulting model does not allow taking into account unpredictable local damage to the windings of induction machines, arising from long-term operation or repair. That is why the actual direction of further research can be considered the improvement of the mathematical apparatus without a significant increase in the input factors for leveling its complexity in practical use.

## 7. Conclusions

1. A mathematical model of an autonomous induction generator with capacitor excitation has been developed when a motor load is connected, taking into account losses in steel and parametric asymmetry in the stator windings. The model makes it possible to comprehensively study electromagnetic and electromechanical processes under various operating modes, including abnormal and emergency modes, the implementation of which on a physical model is difficult or impossible, for example, the influence of parametric asymmetry on the quality of the output voltage of an induction generator, asymmetric loads, emergency modes.

2. The work of an induction generator on consumers with a motor load has been investigated and the starting conditions have been determined for various values of asymmetry in the stator winding of induction machines. It has been found that in transient modes of operation of an induction generator, the parametric asymmetry of its windings manifests itself in a change in the amplitude values of currents (up to 30 %). These factors can be used as diagnostic indicators to monitor such deficiencies in the generator. The influence of the asymmetry of the output voltage of the induction generator on the dynamic characteristics of the induction motor is expressed, first of all, in an increase in the amplitude of the oscillation of the dynamic electromagnetic torque (15–20 %). This negatively affects the operation of both the engine itself and the technological mechanism in which it is used.

3. On the developed thermal mathematical model, which takes into account the coefficient of asymmetry of the stator windings of induction machines, the study of the influence of the asymmetry of the output voltage and its deviation from the nominal value on the heating of the connected induction

motor was carried out. Studies of thermal processes in an induction motor when powered by an induction generator have shown that the asymmetry of the output voltage of an induction generator can reach 3–10 % (which is higher than the permissible 2 %) and causes overheating of the stator windings in excess of the maximum permissible values.

4. Equations were obtained for the temperature rise of the stator winding of an induction motor and the coefficient of unbalance of the voltages of the induction generator as a function of the coefficients of parametric unbalance in the stator windings of the induction generator. An increase in asymmetry in the stator phases of an induction generator and an induction motor by 47.5 % entails an increase in the temperature of the stator winding by 13.9 %. The created regression model made it possible to determine the most rational combination of factors affecting the heating of their stator windings and the quality of the output voltage of the induction generator. On the basis of the equations, the asymmetry coefficient in the electric circuit of the stator phase of an induction generator and an induction motor can be determined, in which the stator windings of machines will not overheat above the maximum permissible temperature values of the corresponding insulation classes. These dependencies make it possible to correctly configure the systems of a variable speed drive when powered from energy sources with induction generators, taking into account the asymmetry of their characteristics.

## Acknowledgement

The results were obtained within the project co-funded by the Polish National Agency for Academic Exchanges (PPN/BUA/2019/1/00016/U/00001).

## References

1. Chorny, O. P., Zachepa, I. V., Mazurenko, L. I., Buryakovskiy, S. G., Chenchevoi, V. V., Zachepa, N. V. (2020). Local autonomous sources of energy supply for emergencies. *Tekhnichna Elektrodynamika*, 5, 45–48. doi: <http://doi.org/10.15407/techned2020.05.045>
2. Chenchevoi, V., Zachepa, I., Chorny, O., Zachepa, N., Ogar, V., Shokarov, D. (2018). The Formed Autonomous Source for Power Supply of Single-Phase Consumers on the Basis of the Three-Phase Asynchronous Generator. 2018 IEEE 3rd International Conference on Intelligent Energy and Power Systems (IEPS), 110–115. doi: <http://doi.org/10.1109/ieps.2018.8559522>
3. Kitsis, S. I. (2003). *Asinkhronnye samovozbuzhdaiuschiesia generatory*. Moscow: Energoatomizdat, 327. Available at: <https://search.rsl.ru/ru/record/01002391609>
4. Toroptsev, N. D. (2004). *Asinkhronnye generatory dlia avtonomnykh elektroenergeticheskikh ustanovok*. Moscow: NTF «Energoprogress», 87. Available at: <https://knigogid.ru/books/1844853-asinkhronnye-generatory-dlya-avtonomnyh-elektroenergeticheskikh-ustanovok>
5. Üçtuğ, Y., Demirekler, M. (1988). Modelling, analysis and control of a wind-turbine driven self-excited induction generator. *IEE Proceedings C Generation, Transmission and Distribution*, 135 (4), 268–275. doi: <http://doi.org/10.1049/ip-c.1988.0037>
6. Hallenius, K.-E., Vas, P., Brown, J. E. (1991). The analysis of a saturated self-excited asynchronous generator. *IEEE Transactions on Energy Conversion*, 6 (2), 336–345. doi: <http://doi.org/10.1109/60.79641>
7. Abbou, A., Barara, M., Ouchatti, A., Akhenaz, M., Mahmoudi, H. (2013). Capacitance required analysis for self-excited induction generator. *Journal of Theoretical and Applied Information Technology*, 55 (3). Available at: [https://www.researchgate.net/publication/287702318\\_Capacitance\\_required\\_analysis\\_for\\_self-excited\\_induction\\_generateur](https://www.researchgate.net/publication/287702318_Capacitance_required_analysis_for_self-excited_induction_generateur)
8. Simoes, M. G., Farret, F. A. (2004). *Renewable Energy Systems: Design and Analysis with Induction Generators*. London: CRC Press, 358. Available at: <https://searchworks.stanford.edu/view/5660475>
9. Zagirnyak, M., Mamchur, D., Kalinov, A. (2014). A comparison of informative value of motor current and power spectra for the tasks of induction motor diagnostics. 2014 16th International Power Electronics and Motion Control Conference and Exposition, 540–545. doi: <http://doi.org/10.1109/epepecm.2014.6980549>
10. Zagirnyak, M., Kalinov, A., Melnykov, V. (2017). Variable-frequency electric drive with a function of compensation for induction motor asymmetry. 2017 IEEE First Ukraine Conference on Electrical and Computer Engineering (UKRCON). Kyiv, 338–344. doi: <http://doi.org/10.1109/ukrcon.2017.8100505>

11. Kuznetsova, Y., Kuznetsov, V., Tryputen, M., Kuznetsova, A., Tryputen, M., Babyak, M. (2019). Development and Verification of Dynamic Electromagnetic Model of Asynchronous Motor Operating in Terms of Poor-Quality Electric Power. 2019 IEEE International Conference on Modern Electrical and Energy Systems (MEES), 350–353. doi: <http://doi.org/10.1109/mees.2019.8896598>
12. Zagirnyak, M., Melnykov, V., Kalinov, A. (2019). The review of methods and systems of fault-tolerant control of variable-frequency electric drives. *Przegląd Elektrotechniczny*, 95 (1), 141–144. doi: <http://doi.org/10.15199/48.2019.01.36>
13. Melnykov, V., Kalinov, A. (2012). The increasing of energy characteristics of vector-controlled electric drives by means of compensation the induction motor parametrical asymmetry. *Technical Electrodynamics*, 3, 85–86. Available at: [http://previous.techned.org.ua/2012\\_3/st40.pdf](http://previous.techned.org.ua/2012_3/st40.pdf)
14. Zagirnyak, M., Kalinov, A., Chumachova, A. (2013). Correction of operating condition of a variable-frequency electric drive with a non-linear and asymmetric induction motor. *Eurocon 2013*. Zagreb, 1033–1037. doi: <http://doi.org/10.1109/eurocon.2013.6625108>
15. Razgildeev, G., Khrantsov, R. (2005). Issledovanie raboty asinkhronnogo generatora na individualnuiu set sredstvami imitatsionnogo modelirovaniia *Vestnik Kuzbasskogo gosudarstvennogo tekhnicheskogo universiteta*, 1, 84–87. Available at: <https://cyberleninka.ru/article/n/issledovanie-raboty-asinhronnogo-generatora-na-individualnuyu-set-sredstvami-imitatsionnogo-modelirovaniya>
16. Kim, C.-W., Jang, G.-H., Seo, S.-W., You, D.-J., Choi, J.-Y. (2020). Experimental verification and analysis of temperature characteristics of induction generator considering stator loss distribution. *AIP Advances*, 10 (1), 015139. doi: <http://doi.org/10.1063/1.5130023>
17. Refoufi, L., Bentarzi, H., Dekhandji, F. Z. (2006). Voltage Unbalance Effects on Induction Motor Performance. *Proceedings of the 6th WSEAS International Conference on Simulation, Modelling and Optimization*. Lisbonm 112–117. Available at: [https://www.academia.edu/3284729/Voltage\\_Unbalance\\_Effects\\_on\\_Induction\\_Motor\\_Performance](https://www.academia.edu/3284729/Voltage_Unbalance_Effects_on_Induction_Motor_Performance)
18. Adouni, A., J. Marques Cardoso, A. (2020). Thermal Analysis of Low-Power Three-Phase Induction Motors Operating under Voltage Unbalance and Inter-Turn Short Circuit Faults. *Machines*, 9 (1), 2. doi: <http://doi.org/10.3390/machines9010002>
19. Zagirnyak, M., Kalinov, A., Melnykov, V., Stakhiv, P. (2016). Fault-tolerant control of an induction motor with broken stator electric circuit. 2016 *Electric Power Networks (EPNet)*. doi: <http://doi.org/10.1109/epnet.2016.7999372>
20. Kuznetsov, V., Tryputen, M., Tytiuk, V., Rozhnenko, Z., Levchenko, S., Kuznetsov, V. (2021). Modeling of thermal process in the energy system “Electrical network – asynchronous motor.” *E3S Web of Conferences*, 280, 05003. doi: <http://doi.org/10.1051/e3sconf/202128005003>
21. Fedorov, M., Ivchenkov, N., Tkachenko, A. (2013). Osobennosti teplovogo sostoianiya asinkhronnykh dvigatelei pri nesimmetrii pitaiushchego napriazheniya. *Nauchniy vestnik Donbasskoi gosudarstvennoi mashinostroitelnoi akademiyi*, 1, 164–170. Available at: [http://nbuv.gov.ua/UJRN/nvdgma\\_2013\\_1\\_25](http://nbuv.gov.ua/UJRN/nvdgma_2013_1_25)
22. Pinchuk, O., Kutkovi, I. (2009). Otsenka teplovogo sostoianiya asinkhronnogo dvigatelja po dannym kontrolja tokov statora pri nesimmetriyi pitaiushchego napriazheniya. *Naukovi pratsi Donetskogo natsionalnogo tekhnicheskogo universitetu*. Serii: *Elektrotehnika i energetika*, 9 (158), 100–196. Available at: [http://ea.donntu.org:8080/bitstream/123456789/5008/1/Art\\_34\\_190.pdf](http://ea.donntu.org:8080/bitstream/123456789/5008/1/Art_34_190.pdf)
23. Pustovetov, M., Sinyavskiy, I. (2011). On dynamics of thermal processes in induction motor under supply voltage unbalance. *Vestnik of Don State Technical University*, 11 (8-1), 1227–1237. Available at: <https://www.vestnik-donstu.ru/jour/article/download/849/844>
24. Zagirnyak, M., Chenchvoi, V., Ogar, V., Yatsiuk, R. (2020). Refining induction machine characteristics at high saturation of steel. *Przegląd Elektrotechniczny*, 96 (11), 119–123. doi: <http://doi.org/10.15199/48.2020.11.24>
25. Kuznetsov, V., Nikolenko, A. (2015). Models of operating asynchronous engines at poor-quality electricity. *Eastern-European Journal of Enterprise Technologies*, 1 (8 (73)), 37–42. doi: <http://doi.org/10.15587/1729-4061.2015.36755>
26. Zagirnyak, M., Prus, V., Rodkin, D., Zachepa, I., Chenchvoi, V. (2019). A refined method for the calculation of steel losses at alternating current. *Archives of Electrical Engineering*, 68 (2), 295–308. doi: <http://doi.org/10.24425/ae.2019.128269>
27. Lv, X., Sun, D., Sun, L. (2019). Determination of Iron Loss Coefficients of Ferromagnetic Materials Used in Cryogenic Motors. 2019 22nd International Conference on Electrical Machines and Systems (ICEMS). doi: <http://doi.org/10.1109/icems.2019.8922160>
28. Liu, G., Liu, M., Zhang, Y., Wang, H., Gerada, C. (2020). High-Speed Permanent Magnet Synchronous Motor Iron Loss Calculation Method Considering Multiphysics Factors. *IEEE Transactions on Industrial Electronics*, 67 (7), 5360–5368. doi: <http://doi.org/10.1109/tie.2019.2934075>
29. Iakimov, V. V. (1996). Problemy ucheta poter v stali pri raschete perekhodnykh protsessov v elektricheskikh mashinakh peremennogo toka. *Tez. dokl. II Mezhdunarodnoi konferentsii po elektromekhanike i elektrotekhnologii*, CHast 1. Krym, 172–174.
30. Iakimov, V. V., Shestakov, A. V. (1997). Uchet poter v stali v sinkhronnykh mashinakh. *Elektrotehnika i energetika*. Kirov, 2, 49–52.
31. Nedelcu, S., Ritchie, E., Leban, K., Ghita, C., Trifu, I. (2013). Iron losses evaluation in soft magnetic materials with a sinusoidal voltage supply. 2013 8th International Symposium on Advanced Topics in Electrical Engineering (ATEE). doi: <http://doi.org/10.1109/atee.2013.6563461>
32. Ionel, D. M., Popescu, M., McGilp, M. I., Miller, T. J. E., Dellinger, S. J., Heideman, R. J. (2007). Computation of Core Losses in Electrical Machines Using Improved Models for Laminated Steel. *IEEE Transactions on Industry Applications*, 43 (6), 1554–1564. doi: <http://doi.org/10.1109/tia.2007.908159>
33. Qiu, Y., Zhang, W., Cao, M., Feng, Y., Infield, D. (2015). An Electro-Thermal Analysis of a Variable-Speed Doubly-Fed Induction Generator in a Wind Turbine. *Energies*, 8 (5), 3386–3402. doi: <http://doi.org/10.3390/en8053386>

34. Hodgins, N., Mueller, M. A., Tease, W. K., Staton, D. (2010). Thermal model of an induction generator in oscillating water column wave energy converter. 5th IET International Conference on Power Electronics, Machines and Drives (PEMD 2010). doi: <http://doi.org/10.1049/cp.2010.0020>
35. Stephen Ejiofor, O., Justin, U., Damian Benneth, N., Uche, O. (2019). Development and thermal modeling of an induction machine. International Journal of Engineering & Technology, 8 (4), 500–508. doi: <http://doi.org/10.14419/ijet.v8i4.29727>
36. Badran, O., Sarhan, H., Alomour, B. (2012). Thermal Performance Analysis of Induction Motor. International Journal of Heat and Technology, 30 (1), 75–88.
37. Shreiner, R. T., Kostylev, A. V., Krivoviaz, V. K., Shilin, S. I. (2008). Elektromekhanicheskie i teplovye rezhimy asinkhronnykh dvigatelei v sistemakh chastotnogo regulirovaniia. Ekaterinburg: GOU VPO “RGPPU”, 361. Available at: <https://www.elibrary.ru/item.asp?id=21333083>
38. Chenchevoi, V., Romashykhin, I., Romashykhina, Z. I., Al-Mashakbeh, A. S. (2017). Analysis of the special features of the thermal process in an induction generator at high saturation of the magnetic system. Electrical Engineering & Electromechanics, 3, 16–18. doi: <http://doi.org/10.20998/2074-272x.2017.3.02>
39. Tryputen, N., Kuznetsov, V., Kuznetsova, Y. (2019). About the Possibility of Researching the Optimal Automatic Control System on a Physical Model of a Thermal Object. 2019 IEEE 2nd Ukraine Conference on Electrical and Computer Engineering (UKRCON), 1244–1248. doi: <http://doi.org/10.1109/ukrcon.2019.8879830>
40. Aarniovuori, L., Lindh, P., Karkkainen, H., Niemela, M., Pyrhonen, J., Cao, W. (2019). Analytical Evaluation of High-Efficiency Induction Motor Losses. 2019 IEEE International Electric Machines & Drives Conference (IEMDC). San Diego, 1501–1507. doi: <http://doi.org/10.1109/iemdc.2019.8785380>
41. EN 50160-2010 (2010). Voltage characteristics of electricity supplied by public distribution networks. Available at: <https://standards.iteh.ai/catalog/standards/clc/18a86a7c-e08e-405e-88cb-8a24e5fedde5/en-50160-2010#:~:text=CLC%2FTFC%208X-,Voltage%20characteristics%20of%20electricity%20supplied%20by%20public%20electricity%20networks,networks%20under%20normal%20operating%20conditions>
42. GOST 13109–97 Elektricheskaia energiiia. Sovmestimost tekhnicheskikh sredstv elektromagnitnaia. Normy kachestva elektricheskoi energii v sistemakh elektrosnabzheniia obshchego naznacheniiia (1999). Minsk: BelGISS, 31. Available at: [http://odz.gov.ua/lean\\_pro/standardization/files/elektromagnitnaja\\_sovmestimost\\_2014\\_03\\_11\\_1.pdf](http://odz.gov.ua/lean_pro/standardization/files/elektromagnitnaja_sovmestimost_2014_03_11_1.pdf)
43. GOST 30804.4.7-2013. Sovmestimost tekhnicheskikh sredstv elektromagnitnaia. Obshee rukovodstvo po sredstvam izmerenii i izmereniyam garmonik i intergarmonik dlia sistem elektrosnabzheniia i podkliuchaemykh k nim tekhnicheskikh sredstv (2013). Moscow: Standartinform. Available at: <https://shop.znak.store/gost/oks-33/oks-33-100/oks-33-100-10/gost-30804472013-iec-61000472009-sovmestimost-tehnicheskikh-sredstv-elektromagnitnaya-obshee-rukovodstvo-po-sredstvam-izmerenij-i-izmereniyam-garmonik-i-intergarmonik-dlya-sistem-elektrosnabzheniya-i-p>
44. Sistemy elektricheskoi izoliatsiyi. Otsenka nagrevostoikosti i klassifikatsiya: GOST 8865-93 (1993). Kyiv: Gosstandart Ukrainy, 14.
45. Adler, Iu. P., Markova, E. V., Granovskii, Iu. V. (1976). Planirovanie eksperimenta pri poiske optimalnykh usloviy. Moscow: Nauka, 279.
46. Borovikov, V. (2003). STATISTICA. Iskusstvo analiza dannykh na kompiutere: Dlia professionalov. Saint Petersburg: Piter, 688.
47. Chenchevoi, V., Zacheva, I., Chornyi, O., Chencheva, O., Yatsiuk, R. (2020). Electric Power Quality Induction Generator with Parametric Asymmetry. 2020 IEEE KhPI Week on Advanced Technology (KhPIWeek), 504–508. doi: <http://doi.org/10.1109/khpiweek51551.2020.9250097>